Blowout from a hydrogen storage cavern

Hippolyte Djizanne, Benoit Brouard, Pierre Bérest, Grégoire Hévin, Carlos Murillo Rueda

BLOWOUT FROM A HYDROGEN STORAGE CAVERN

Hippolyte Djizanne[(1)], Benoit Brouard[(2)], Pierre Bérest[(3)],
Grégoire Hévin[(4)] & Carlos Murillo Rueda[(1)]

[(1)] Ineris, Parc Technologique ALATA, BP 2, 60550 Verneuil-en-Halatte, France

[(2)] Brouard Consulting, 101 Rue du Temple, 75003 Paris, France

[(3)] LMS, Ecole Polytechnique, Route de Saclay, 91128 Palaiseau, France

[(4)] Storengy, 12 Rue Raoul Nordling, 92270 Bois-Colombes, France

Abstract

To prevent catastrophic climate change, Europe and the world must rapidly shift to low carbon and renewable energies. Hydrogen as an energy vector, provides viable solutions to replace polluting and carbon-emitting fossil fuels. Gaseous hydrogen can be stored in underground storage and coupled with the existing natural gas pipe networks.

Storage in salt caverns was recognized to be the best suited technology to meet new energy system challenges. Hydrogen storage caverns are currently operated in the UK and in Texas. A preliminary risk analysis dedicated to underground hydrogen salt cavern highlights the importance of containment losses (leaks) but also of the formation of a gas cloud following a blowout whose ignition may generate dangerous phenomena such as jet fire, Unconfined Vapor Cloud Explosion (UVCE) or flashfire as well. A blowout is one of the major accidental scenarios likely to occur during the operation of a hydrogen underground storage in salt cavern. Blowout is an uncontrolled release of gas from well after pressure control systems have failed. Several examples of blowouts in gas storage caverns have been described in the literature, such as that in an ethane storage at Fort Saskatchewan, Canada (Alberta Energy and Utilities Board, 2002) or in a natural gas storage at Moss Bluff, Texas (Rittenhour and Heath, 2012), see Réveillère et al., 2017.

This paper presents the modeling of the subterraneous and aerial parts of a blowout from a hydrogen storage cavern. In the first part of this article, the method presented in Bérest et al. (2013) is used to predict the duration of the eruption and the evolution of key thermodynamics parameters such as hydrogen temperature, pressure, velocity and density. Then these results are used to compute dispersion in the atmosphere of the hydrogen jet outflowing from the wellhead and to evaluate the effects of potential resulting phenomena on surrounding assets.

Key words: Hydrogen, Blowout, Salt caverns, Computer modeling, Thermodynamics, Flash fire, UVCE, Jet fire.

Context

The decarbonation of energy is a main priority in Europe. At least 40% cuts in greenhouse gas emissions and a 32% share for renewable energy are to be achieved in 2030. However, 65% of Europe's energy demand is still met by natural gas, coal, and other fossil fuels.

Beyond the challenges related to the production of this hydrogen in large quantities, it is essential to ensure the safety of hydrogen underground storage which will be used to guarantee the continuity of services i.e., as a buffer energy storage in support of intermittent sources of renewable energy. Geological hydrogen storage, based on the example that has been developed for natural gas, - by providing seasonal capacity - can be a key solution to foster the decarbonization of energy by making renewable hydrogen available at any time for mobility, industry and household heating uses.

Several studies have benchmarked underground storage types based on their characteristics. Salt cavern storage was recognized to be the best suited technology to meet new European energy system challenges. Salt caverns created by solution mining offer the advantage of being virtually impermeable to gases and are currently the only structures used to massively store hydrogen underground. In recent decades, underground hydrogen storage salt caverns have emerged and are already in operation in the U.K. and the U.S.A:

- In Teesside in the United Kingdom, where for more than 30 years, 3 salt caverns whose geometrical volume is 70,000 m^3 (*0.6 MMbbls*) each, have been in operation. Each can store 1 million Nm^3 of almost pure hydrogen (95% H_2 and 3-4% CO_2). These salt caverns are located at an average depth of 370 m (*1,214 ft*).
- At Clemens Dome, Lake Jackson in Texas (USA) where, since 1986, Conoco Philips has stored 30.2 Mm^3 (*254 MMbbls*) of hydrogen from synthesis gas (95% hydrogen) in an 850 m (*2,800 ft*) depth salt cavern. The salt cavern has a geometric volume of 580,000 m^3 and is operated between 70-135 bar (1,105-1,958 psi) with a minimum calorific value of 92 MWh.
- In Moss Bluff, Liberty County, Texas, where, since 2007, Praxair has stored 70.8 Mm^3 (*594 MMbbls*) of industrial hydrogen in a salt cavern. The cavern has a geometric volume of 566,000 m^3 (*4.7 MMbbls*) and is operated between 76 bar (*1,102 psi*) and 134 bar (*1,944 psi*) with a minimum calorific value of 80 GWh.
- At Spindletop Dome, in Beaumont, Texas (USA), Air Liquide recently commissioned the largest underground hydrogen storage facility in a salt cavern in the world. The salt cavern is located at a depth of 1,500 m (*4,922 ft*) and its diameter is about 70 m (*230 ft*).

These storage facilities have demonstrated the feasibility of storing hydrogen in salt caverns.

Introduction

Several studies are underway around the world on the underground storage of hydrogen gas. For example, the European HyPSTER project (2021-2023) aims at demonstrating the feasibility of operating underground hydrogen storage in salt caverns on an industrial scale. In this context, a pilot site is planned in France, at Bresse Vallons (Ain) on the EZ53 cavern, which is one of the most studied salt caverns in France.

This paper focuses on the blowout modeling on a hydrogen storage cavern. A blowout is one of the major accidents feared in such industrial site (TNO, 2020). A small number of blowouts from gas storage caverns (for example, at Moss Bluff, Texas and Fort- Saskatchewan, Canada, see Réveillère et al., 2017, were described in the literature. Gas flow lasted several days before the caverns were empty. It is generally considered that in Europe, where implementing of a SSSV (Subsurface Safety Valve) is mandatory in all gas storage caverns, the probability of occurrence of such an incident is divided by several orders of magnitude.

An important aspect of blowout modeling is the ability to accurately predict the mass flow rate of gas exiting the wellhead by simulating a turbulent Fanno-type flow: an option that does not appear to be available in most software used in the industry to predict a blowout. Bérest et al. (2013) provided a simplified method that allows computing blowout duration and evolution of gas temperature and pressure in the cavern and in the well. The thermodynamic model of the cavern is able to explain correctly the evolution of cavern gas temperature during a (controlled) gas withdrawal; duration of the Moss Bluff blowout can be back-calculated correctly; and the computed air velocities are compatible with the ballistic flight of bricks observed during the Kanopolis blowout, as was proved by Van Sambeek (2009).This method was implemented in LOCAS software to allow fully coupled (Thermo-Hydro-Mechanical) numerical computations of the underground part of a blowout scenario in gaseous salt cavern (hydrogen, compressed air, and natural gas for example). The first part of this paper presents the result of blowout numerical computations on a typical cavern plus a sensitivity analysis on key parameters such as well length, production tubing diameter, stored gas, and cavern volume.

As a major accidental scenario, the severity of consequences of inflammations of hydrogen leakages during a blowout from a hydrogen storage cavern is assessed in the second part of this paper. Standard models for gas dispersion are used with reasonably safe hypotheses on the source terms (dimension of the breach, initial pressure, volume of gas available) and on the jet orientation (vertical). For the numerical description of a blowout scenario, a set of 2D simulations is developed to predict the main characteristics of the combustible cloud formed during the dispersion process. Then, the results of the computational description of the hydrogen atmospheric dispersion are considered for assessing thermal and overpressure effects with complementary computational tools.

Underground blowout prediction model

Bérest's model integrates the thermodynamics of gas in the well-cavern system to predict the values of the main parameters during a blowout from an underground gas storage caverns. Only major assumptions and simplifications of the model are provided in this section. More details can be found in Bérest et al., 2013, Djizanne et al., 2014.

Cavern gas thermodynamic behavior

Both gas behaviors in the cavern and in the wellbore must be described; they are coupled through the boundary conditions at gas entry from the cavern to the string (gas temperature and pressure must be continuous). The thermodynamic behavior of hydrogen exhibits some specific features of interest (in particular, an isenthalpic depressurization can lead to hydrogen warming); so, instead of the standard state equation of an ideal gas, a van der Waals state equation was selected to describe the gas behavior during the blowout, $P = -a/v^2 + RT/(v-b)$ and $h(v,T) = C_v T - 2a/v + rTv/(v-b)$ (*P*, *T* and *v* are gas pressure, temperature and specific volume; $h = e + Pv$ is the gas enthalpy). However, ideal gas state equation is used for natural gas such as methane or compressed air.)

During a gas withdrawal, the energy balance equation can be written $d\left[m(\dot{e}(T,v)+P\dot{v})\right]/dt = Q$ where m is the mass of gas in the cavern, e is the gas internal energy. In addition, cavern volume is constant, or $V = mv$. From Thermodynamics, $\dot{e}(T,v)+P\dot{v} = C_v\dot{T} + T(\partial P/\partial T)_v\dot{v}$. Q is the heat flux transferred from the rock mass to the cavern gas through the cavern wall. Blowout from a gas cavern is a rapid process: it is completed within a week or less. During such a short period of time, temperature changes are not given time enough to penetrate deep into the rock mass and, from the perspective of thermal conduction, cavern walls can be considered as the sum of small flat surfaces whose area equals the actual area of the cavern, or Σ_c.

When a varying temperature, $T_c = T_c(t)$, is applied on the surface, the heat flux per surface unit can be expressed as $Q = \Sigma_c\int_0^t -K\dot{T}_c(\tau)d\tau/\sqrt{\pi k(t-\tau)}$ where K = 6 W/m-K and k = 3 10^{-6} m^2 are the thermal conductivity and diffusivity of salt, respectively. When these simplifications are accepted, the heat balance equation can be written:

$$\frac{\dot{T}_c}{v} + (\gamma-1)\frac{\dot{v}T_c}{v^2} = \frac{-\Sigma_c K}{C_v V\sqrt{k}}\int_0^t \frac{\dot{T}_c(\tau)}{\sqrt{\pi(t-\tau)}}d\tau$$

This equation allows computing T, P, v in the cavern when mass evolution $m = m(t)$ is known.

Gas thermodynamic behavior in the wellbore.

The gas rate in the borehole is a couple hundreds of meters per second, typically (more when hydrogen is considered). This means that only a few seconds are needed for gas to travel from the cavern top to ground level. Such a short period of time is insufficient for cavern pressure to experience large changes and steady state can be assumed at each instant. (Obviously, when longer periods of time are considered, cavern pressure slowly decreases). Duct diameter or D is assumed to be constant throughout the well; hence, the cross-sectional area of the well is constant too. Gas massic flowrate is $\dot{m} = u/v$. Enthalpy is such that $dh/dz + udu/dz + g = 0$ (Bernoulli). The momentum equation can write $vdP/dz + vdv/dz + g = -f(u)$. Head losses per unit of length are described by $f(u) > 0$. During the blowout, the gas flow is turbulent. The effects of friction are confined to a thin boundary layer at the steel casing wall. The average gas velocity is uniform through any cross-sectional area (except, of course, in the boundary layer). For simplicity, head losses are written $f(u) = Fu^2$ where $F = f/2D$ is the friction coefficient and f is the friction factor. The Cole brook's equation is used, $1/\sqrt{f} = -2\log_{10}(\varepsilon/3.71D)$ where ε is the well roughness (ε = 0.02 mm is typical).

Gas pressure and temperature (hence, gas specific volume) at the end of the string are known from the computation of cavern gas thermodynamic behavior. In principle, gas pressure at the wellhead should be atmospheric. However, when gas flow rate is very high, such an assumption leads to a solution such that gas flow is supersonic in the upper part of the well, which is not compatible with the second principle of thermodynamics ($dS/dz > 0$) [no shock can exist inside the wellbore]. In such a case, it is assumed that the flow rate is sonic at the wellhead ("choked flow"), or $u = c$. No constraint is applied to wellhead gas pressure which, in general, is larger than atmospheric. Conversely, when the cavern pressure is relatively small, the gas flow is said to be "normal" and gas pressure is atmospheric at ground level. These assumptions ("Fanno-flow" model) are standard (Landau and Lifschitz, 1971, Section 91) and are commonly accepted (Von Vogel and Marx, 1985).

Note that heat transfer from the rock mass to the wellbore, or from the brine sump to the cavern gas body, are neglected. In the computations, gravity forces (g) are neglected. This model was tested against the Moss Bluff historical case with good results (blowout duration was predicted correctly.)

Description of studied caverns

Caverns geometrical properties

This paper presents the results of the blowout numerical computation performed on 3 generic salt caverns (Cavern#0, Cavern#1 and Cavern#2, see Figure 1). All the caverns are supposedly cylindrical, and their main properties are presented in Table 1. Large and deep caverns (volume larger than 100,000 m^3 or 0.8 MMbbls and casing-shoe, depth equal to 1,000 m or 3,281 ft) are considered. Caverns parameters selected for numerical computations are presented in Table 2.

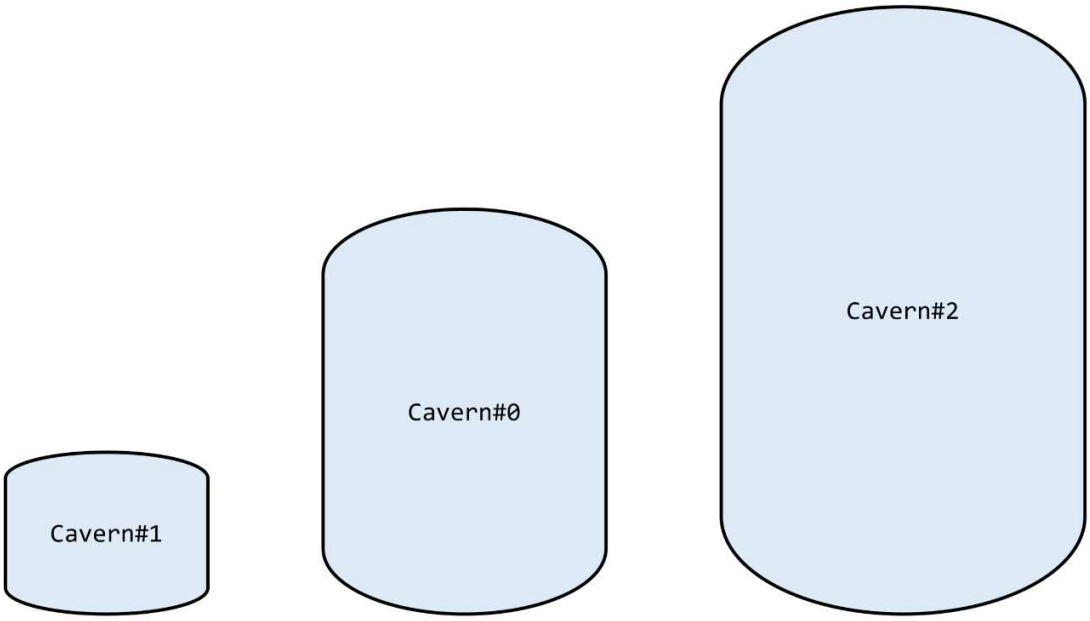

Figure 1. Vertical cross section of the 3 generic hydrogen storage caverns (Cavern#0, Cavern#1 and Cavern#2) for which a blowout analysis is carried out.

To ensure the tightness of the storage, a double-packer completion is set in the wellbore and the maximum gas pressure is not higher than 80-85% of the geostatic pressure at the casing-shoe depth (Bérest et al. 2021). For all these caverns, the blowout scenario includes a wellhead failure; however, the production tubing stays in place during cavern emptying through the well. At the beginning of the blowout, the initial pressure is very close to the maximum operating pressure.

Table 1. Salt cavern properties for blowout numerical computations.

Blowout Keys parameters (Hydrogen)	Cavern#1	Cavern#0	Cavern#2
Gas initial pressure at cavern top	16.6 MPa *2,409 psi*	17.6 MPa *2,551 psi*	18.2 MPa *2,644 psi*
Gas initial temperature in the cavern	45°C *113°F*	45°C *113°F*	45°C *113°F*
Well length – cavern top depth	1,000 m *3,281 ft*	1,000 m *3,281 ft*	1,000 m *3,281 ft*
Tubing diameter – internal diameter	7"5/8 *0.17 m*	8"5/8 *0.20 m*	9"5/8 *0.22 m*
Roughness (ε)	0.02 mm *0.0008 in*	0.02 mm *0.0008 in*	0.02 mm *0.0008 in*

Cavern total height	68 m *223 ft*	197 m *646 ft*	284 m *932 ft*
Cavern diameter	50 m *164 ft*	60 m *196 ft*	70 m *229 ft*
Cavern volume	100,793 m^3 *0.8 MMbbls*	500,456 m^3 *4.2 MMbbls*	1,003,163 m^3 *8.4 MMbbls*
Cavern overall surface (m^2)	10,681 m^2 114,928 ft^2	37,134 m^2 399,562 ft^2	62,455 m^2 672,016 ft^2

Cavern#0 represents the typical dimensions for hydrogen storage caverns with a cavern volume ~ 500,000 m^3 (*4.2 MMbbls*) and pressure range between 60 and 180 bars (*870 – 2,610 psi*).

Secondly, a sensitivity analysis is performed on several parameters such as the well length, the well diameter, gas type and the salt cavern volume (see Table 4). The first three sensitivity analyzes (well length, well diameter and gas type) are carried out on the Cavern#0. The other two caverns (Cavern#1 and Cavern #2) are used for the last sensitivity analysis where three (03) salt caverns with different volumes and different tubing diameters are all positioned at a 1,000-m (*3,281 ft*) depth (see Table 2).

Table 2. Parameters of the blowout sensitivity analysis

Blowout sensitivity analysis parameters			
Well length (*cavern top depth*)	250 m *820 ft*	1,000 m 3,281 ft	1,500 m 4,922 ft
Tubing diameter (*Internal diameter*)	*7"5/8* *0.17 m*	*8"5/8* *0.20 m*	*9"5/8* *0.22 m*
Different Gas blowout	Methane	Hydrogen	Compressed Air
Caverns at the same roof depth	Cavern#1	Cavern#0	Cavern#2

Gas thermodynamic properties

Gas properties used in this paper are presented in Table 3 (from Gas Encyclopedia, Air Liquide, 2012; pressure and temperature are 10^5 Pa or *14.7 psi* and 298.15 K or *77°F*, respectively). Normal conditions m^3(n) or Nm^3, are defined as follows: 0°C = 32 °F and 1 atm = 1.01325 bar = 14.7 psi (Table 4).

Table 3. Gas constants.

Gas	C_p (J/kg.K) *(BTU/lb/°F)*	C_v (J/kg.K) *(BTU/lb/°F)*	γ(-)	M (g/mol) *(lbm/mol)*	a ($J.m^3/kg^2$)	b (m^3/kg)
Methane	2,237 *534*	1,714 *409.3*	1.305	16.043 *0.035*	-	-
Hydrogen	14,831 *3,542*	10,714 *2,558*	1.384	2.016 *0.004*	6,092	0.013
Compressed Air	1,010 *241*	719 *171.7*	1.402	28.95 *0.064*	-	-

Table 4. Gas properties of hydrogen and natural gas.

Gas properties	Methane	Hydrogen
Density (normal conditions)	0.7893 kg/m^3 0.0492 lb/cft	0.0899 kg/m^3 0.00561 lb/cft
HHV Higher heating value (per volume)	11.40 kWh/m^3 (n) 38,898 BTU/m^3 (n)	3.3 kWh/m^3 (n) 10,236 BTU/m^3 (n)
HHV Higher heating value (per mass)	14.4 kWh/kg 0.802 MMBTU/m^3 (n)	36.7 kWh/kg 2.044 MMBTU/m^3 (n)

Results of the computation of the blowout subterraneous evolution

This section discusses the result of the blowout simulation of generic hydrogen storage caverns. First, the results of the typical Cavern#0 are presented and commented. Secondly, the results of the sensitivity analysis are provided. Discussion on the numerical results mainly focuses on blowout duration, gas rates at ground level and the evolutions of gas temperature and pressure in the cavern.

Cavern#0 results

This section details the evolution of the thermodynamic parameters that characterize gas flow from Cavern#0 to the surface (ground level). Cavern#0 is a 500,456 m^3 (*4.2 MMbbls*) cylindrical salt cavern.

Figure 2 shows the evolution of hydrogen mass as a function of time during the blowout. Hydrogen mass in the cavern decreases smoothly. The heat flux provided by the rock mass is especially high after 1 day (26 MW or *25,155 BTU/s*, see Figure 2*b*).

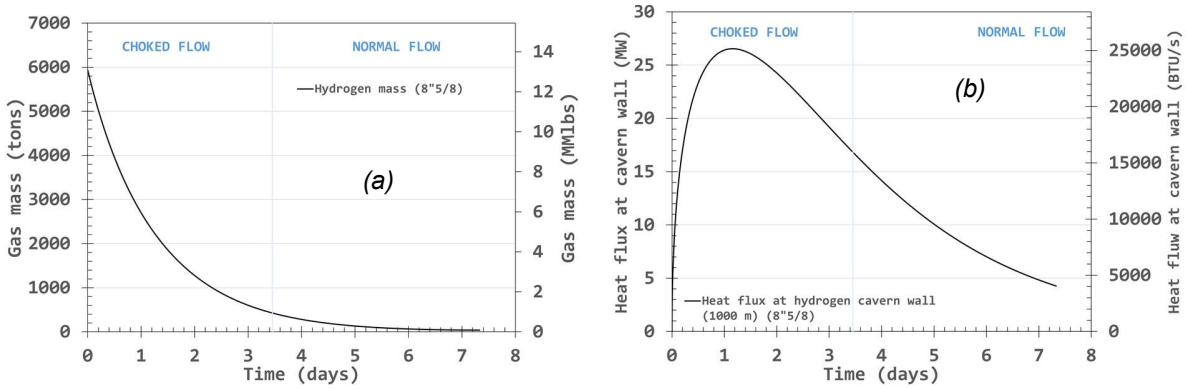

Figure 2. Evolution of *(a)* hydrogen mass and *(b)* heat flux at salt cavern wall as a function of time

The blowout is approximately 7.3-day long in Cavern#0. Hydrogen flow is choked (gas velocity is sonic at the wellhead) during the first 3.4 days and normal during the second half of the blowout. Figure 3 successively displays: a) hydrogen pressure in the cavern and hydrogen depressurization in the well; b) hydrogen temperature in the cavern and outlet temperature; c) hydrogen density at cavern top and at the ground level and d) hydrogen velocity.

Hydrogen pressure in the cavern is 17.6 MPa (*2,551 psi*) when the blowout starts and drops to 0.1 MPa (*14.7 psi*) after 7.3 days (Figure 3*a*). Gas depressurization in the well is intense, and wellhead pressure is small even during the choked part of the blowout. Later during the normal flow, the cavern gas pressure becomes much smaller, resulting in slower velocities and normal flow.

The most important parameter is hydrogen temperature (Figure 3*b*). In Cavern#0, it plummets from 45 °C (*113 °F*) to 1.19 °C (*34 °F*), a temperature reached after 1.3 day. Heat flux at this time is so large (see Figure 2b) that hydrogen warms again to reach 38°C (*100 °F*) in the cavern at the end of the blow-out. Except at the end of the blowout, the gas temperature at ground level temperature is much colder than the cavern temperature.

Hydrogen velocity is high (Figure 3d); it equals the speed of sound at ground level, where the flow is choked. Note that sound celerity in hydrogen (more than 1,200 m/s or *3,937 ft/s*) is much faster than in air or natural gas. Gas velocities drastically drop when the flow regime changes from choked to normal.

The “end” of the blowout is a difficult notion to define. The thermal equilibrium between cavern gas and rock mass should ideally be reached. After choked flow ends, the cavern gas slowly warms, resulting in a low gas outflow rate of approximately 6 m/s (*20 ft/s*); the pressure difference between the cavern and ground level is no longer the driving force of the gas flow.

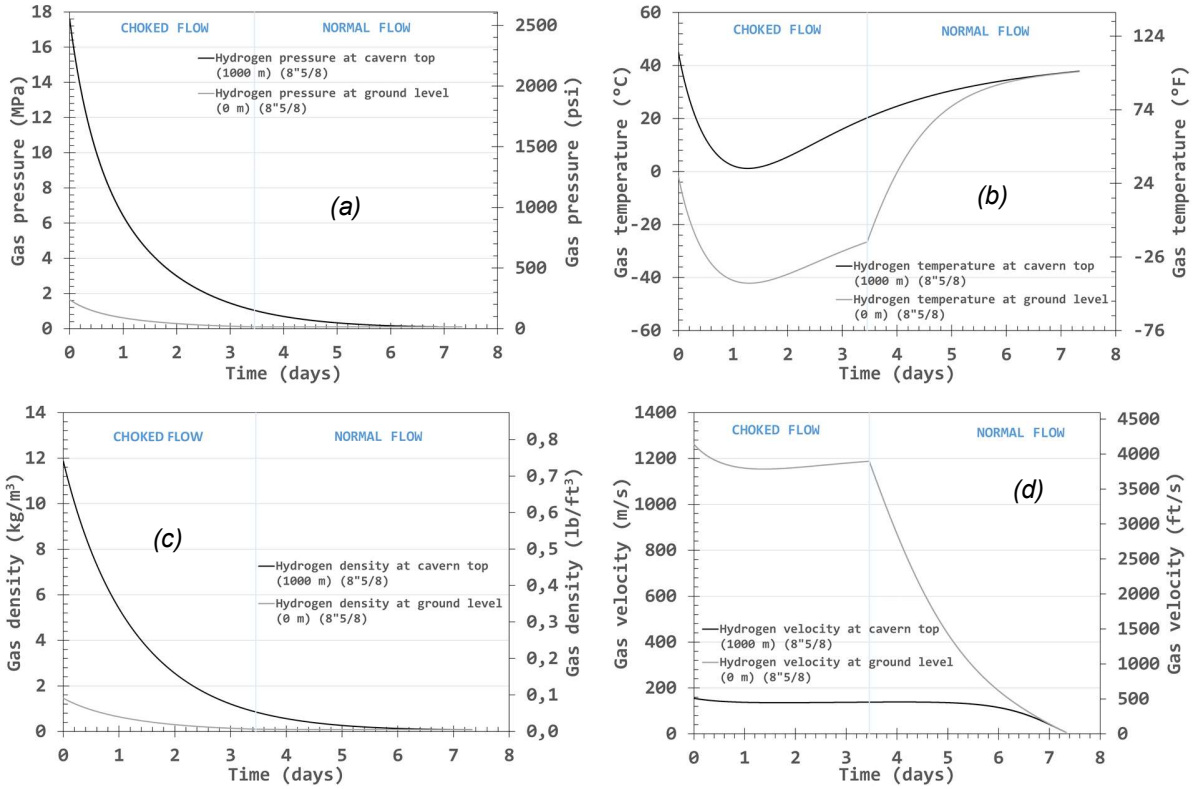

Figure 3. Evolution of hydrogen pressure *(a)*, hydrogen temperature *(b)*, hydrogen density *(c)* and hydrogen velocity *(d)* as a function of time.

Figure 4 shows the distribution of *(a)* hydrogen pressure and *(b)* hydrogen temperature as a function of depth at the beginning of the blowout (*t*=0). The distribution of the temperature through the well from the cavern top to ground level (Figure 4*b*) highlights the significance of the Joule-Thompson effect (see section related to the Joule-Thompson effect). Indeed, when the velocities at the base of the well are low, enthalpy remains almost constant, hydrogen temperature increases in the well, an effect that is not captured when the state equation of gas is ideal.

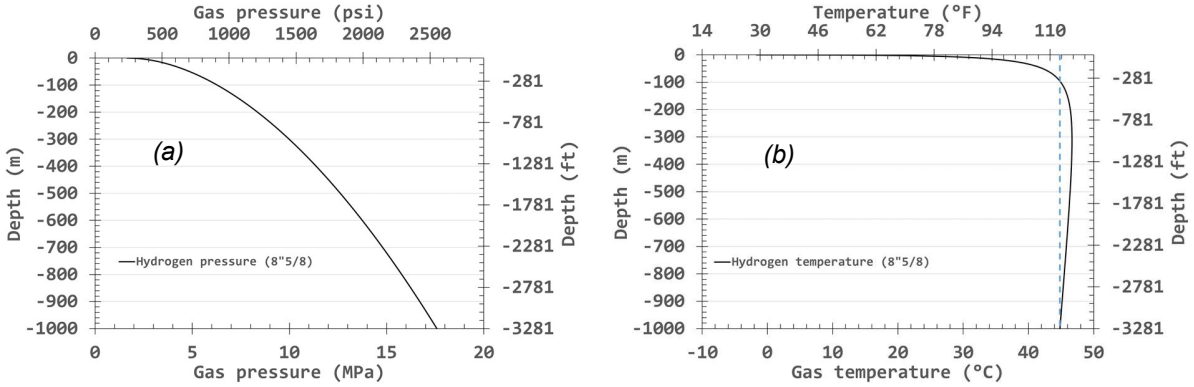

Figure 4. Distribution of pressure *(a)* and hydrogen temperature *(b)* as a function of depth at the starts of the blowout *(t=0).*

Summary of the results of the blowout on Cavern#0 are provided on Table 5. These results of the Cavern#0 are exploited in the second part of this paper to model the aerial part of the blowout.

Table 5. Summary of the results of blowout analysis on Cavern#0.

Blowout Keys parameters	Cavern#0
Blowout duration	7.3 days
Choked flow duration	3.4 days
Normal flow duration	3.9 days
Gas initial pressure	17.6 MPa *2,551 psi*
Ground level pressure at the start of the blowout	1.65 MPa *239 psi*
Cavern top pressure at the end of the choked flow	1.04 MPa *150 psi*
Ground level pressure at the end of the choked flow	0.10 MPa *14.7 psi*
Gas initial temperature	45°C *113°F*
Ground level temperature at the start of the blowout	-1.69°C *29 °F*
Gas temperature at cavern top at the end of the choked flow	20°C *69°F*
Ground level temperature at the end of the choked flow	-27°C -16 °F
Lowest temperature in the cavern	1.2 °C 34 °F
Lowest temperature at ground level	-42 °C -44 °F
Well length or cavern top depth	**1,000 m** ***3,281 ft***
Gas velocity at cavern top at the start of blowout	155 m/s *509 ft/s*
Gas velocity at ground level at the start of blowout	1,262 m/s *4,142 ft/s*
Gas velocity at cavern top at the end of the choked flow	138 m/s *453 ft/s*
Gas velocity at ground level at the end of the choked flow	1,187 m/s *3,897 ft/s*
Cavern volume	**500,456 m^3** ***4.2 MMbbls***
Gas mass	5,936 tons *13 MMlbm*
Maximum flux from cavern wall	26 MW *25,155 BTU/s*
Tubing diameter (internal diameter)	**8"5/8** ***0.20 m***

Analysis of sensitivity to well length

Table 6 presents a summary of the results of blowout sensitivity analysis to well length. In this analysis, Cavern#0 is positioned at 3 different depths: 250 m (*820 ft*), 1,000 m (*3,281 ft*) and 1,500 m (*4,922 ft*). Hydrogen pressure and temperature vary, as hydrogen mass, but the tubing diameter is fixed at 8"5/8. It is observed that the longer the well, the greater the blowout duration. The minimum temperatures at ground level and in the cavern are reached in the 1,000-m (3,281 ft) long tubing. During the first part of the blowout, when the flow is choked, the highest gas velocities at the ground level and the lowest gas velocities at the cavern top are those of the 1,500 m well (*4,922 ft*).

Table 6. Summary of the results of blowout sensitivity analysis on well length.

Blowout Keys parameters	Shallow	Mean	Deep
Blowout duration	3.0 days	7.3 days	9.2 days
Choked flow duration	1.4 days	3.4 days	4.3 days
Normal flow duration	1.6 days	3.9 days	4.9 days
Gas initial pressure	4.4 MPa *637 psi*	17.6 MPa *2,551 psi*	26.4 MPa *3,827 psi*
Ground level pressure at the starts of the blowout	0.8 MPa *115 psi*	1.7 MPa *239 psi*	2 MPa *291 psi*
Cavern top pressure at the end of the choked flow	0.6 MPa *80 psi*	1.04 MPa *151 psi*	1.3 MPa *183 psi*
Ground level pressure at the end of the choked flow	0.1 MPa *14.7 psi*	0.1 MPa *14.7 psi*	0.1 MPa *14.7 psi*
Gas initial temperature	25°C *77°F*	45°C *113°F*	60°C *140°F*
Ground level temperature at the starts of the blowout	-21°C *-38°F*	-1.7°C *29°F*	14°C *58°F*
Gas temperature at cavern top at the end of the choked flow	9°C *48°F*	20°C *69°F*	32.51°C *91°F*
Ground level temperature at the end of the choked flow	-34.88°C *-31°F*	-26.53°C *-16°F*	-16°C *29°F*
Lowest temperature in the cavern	2.7°C *37°F*	1.2°C *34°F*	7.8°C *46°F*
Lowest temperature at ground level	-40°C *-40°F*	-42°C *-44°F*	-36°C *-33°F*
Well length or cavern top depth	**250 m** ***820 ft***	**1,000 m** ***3,281 ft***	**1,500 m** ***4,921 ft***
Gas velocity at cavern top at the starts of blowout	265 m/s *869 ft/s*	155 m/s *509 ft/s*	135 m/s *445 ft/s*
Gas velocity at ground level at the starts of blowout	1,208 m/s *3,965 ft/s*	1,262 m/s *4,142 ft/s*	1,302 m/s *4,274 ft/s*
Gas velocity at cavern top at the end of the choked flow	253 m/s *831 ft/s*	138 m/s *453 ft/s*	116 m/s *382 ft/s*
Gas velocity at ground level at the end of the choked flow	1,167 m/s *3,830 ft/s*	1,187 m/s *3,897 ft/s*	1,212 m/s *3,976 ft/s*
Cavern volume	500,456 m^3 *4.2 MMbbls*	500,456 m^3 *4.2 MMbbls*	500,456 m^3 *4,2 MMbbls*
Gas mass	1,736 tons *4 MMlbm*	5,936 tons *13 MMlbm*	8,028 tons *18 MMlbm*
Maximum flux from cavern wall	18MW *17,127 BTU/s*	26MW *25,155 BTU/s*	29.65 MW *28,102 BTU/s*
Tubing diameter – internal diameter	8"5/8 *0.20 m*	8"5/8 *0.20 m*	8"5/8 *0.20 m*

Analysis of sensitivity to tubing diameter

For this sensitivity analysis, Cavern#0 roof is positioned at a 1,000-m (*3,281 ft*) depth, and the effect of 3 different tubing diameters on the emptying of the cavern is analyzed. It is observed that the larger the diameter, the faster the salt cavern empties and the larger is the gas temperature drop. Hydrogen velocities at ground level are higher at the start of the blowout for the cavern with the largest tubing. Summary of the results of the blowout sensitivity analysis on tubing diameter is provided on Table 7.

Table 7. Summary of the results of blowout sensitivity analysis on tubing diameter.

Blowout Keys parameters	Small	Medium	Large
Blowout duration	10.5 days	7.3 days	5,6 days
Choked flow duration	4.8 days	3.4 days	2.7 days
Normal flow duration	5.7 days	3.9 days	2.9 days
Gas initial pressure	17.6 MPa *2,551 psi*	17.6 MPa *2,551 psi*	17.6 MPa *2,551 psi*
Ground level pressure at the starts of the blowout	1.5 MPa *220 psi*	1.7 MPa *239 psi*	1.8 MPa *254 psi*
Cavern top pressure at the end of the choked flow	1.12 MPa *162 psi*	1.04 MPa *151 psi*	0.98 MPa *142 psi*
Ground level pressure at the end of the choked flow	0.10 MPa *14.7 psi*	0.10 MPa *14.7 psi*	0.10 MPa *14.7 psi*
Gas initial temperature	45°C *113°F*	45°C *113°F*	45°C *113°F*
Ground level temperature at the starts of the blowout	-1.7°C *29°F*	-1.7°C *29°F*	-1.7°C *29*
Gas temperature at cavern top at the end of the choked flow	25°C *78°F*	20°C *68°F*	16°C *60°F*
Ground level temperature at the end of the choked flow	-22°C *-8°F*	-27°C *-16°F*	-30°C *-22°F*
Lowest temperature in the cavern	7.6°C *46°F*	1.2°C *34°F*	-4.09°C *25°F*
Lowest temperature at ground level	-37°C *-34°F*	-42°C *-44°F*	-47°C *-55°F*
Well length or cavern top depth	1,000 m *3,281 ft*	1,000 m *3,281 ft*	1,000 m *3,281 ft*
Gas velocity at cavern top at the starts of blowout	143 m/s *469 ft/s*	155 m/s *509 ft/s*	165 m/s *541 ft/s*
Gas velocity at ground level at the starts of blowout	1,261 m/s *4,138 ft/s*	1,263 m/s *4,142 ft/s*	1,264 m/s *4,145 ft/s*
Gas velocity at cavern top at the end of the choked flow	129 m/s *422 ft/s*	138 m/s *453 ft/s*	146 m/s *478 ft/s*
Gas velocity at ground level at the end of the choked flow	1,198 m/s *3,930 ft/s*	1,188 m/s *3,897 ft/s*	1,179 m/s *3,867 ft/s*
Cavern volume	500,456 m^3 *4.2 MMbbls*	500,456 m^3 *4.2 MMbbls*	500,456 m^3 *4.2 MMbbls*
Gas mass	5,936 tons *13 MMlbm*	5,936 tons *13 MMbls*	5,936 tons 13 MMlbm
Maximum flux from cavern wall	21 MW *19,714 BTU/s*	27 MW *25,155 BTU/s*	32 MW *30,187 BTU/s*
Tubing diameter – internal diameter	***7"5/8*** **0.17 m**	***8"5/8*** **0.20 m**	***9"5/8*** **0.22 m**

Analysis of sensitivity to gas nature (methane, hydrogen and compressed air)

For this sensitivity analysis, gas pressure in Cavern#0 is the maximum operating pressure; the cavern is filled with methane, hydrogen or compressed air (see Table 8). A comparison is done on the gas behaviors during their flows from salt cavern to the wellhead through the wellbore. The blowout from a compressed air cavern is slower than from methane or hydrogen caverns. The fastest blowout is that of the salt cavern filled with hydrogen because hydrogen viscosity is smaller than natural gas viscosity. Not to mention that hydrogen is approximately 8 times "lighter" than natural gas (Louvet et al., 2017). During the blowout, the largest gas cooling is measured in the hydrogen salt cavern.

Table 8. Summary of the results of blowout sensitivity analysis on 3 gases.

Blowout Keys parameters	Methane	Hydrogen	Compressed Air
Blowout duration	21 days	7.3 days	25.5 days
Choked flow duration	10.5 days	3.4 days	13.8 days
Normal flow duration	10.5 days	3.9 days	11.6 days
Gas initial pressure	17.6 MPa *2,551 psi*	17.6 MPa *2,551 psi*	17.6 MPa *2,551 psi*
Ground level pressure at the starts of the blowout	1.8 MPa *260 psi*	1.6 MPa *239 psi*	1.7 MPa *245 psi*
Cavern top pressure at the end of the choked flow	0.99 MPa *144 psi*	1.04 MPa *151 psi*	1.05 MPa *152 psi*
Ground level pressure at the end of the choked flow	0.10 MPa *14.7 psi*	0.10 MPa *14.7 psi*	0.10 MPa *14.7 psi*
Gas initial temperature	45°C *113°F*	45°C *113°F*	45°C *113°F*
Ground level temperature at the starts of the blowout	3 °C *38°F*	-2°C *29°F*	-8°C *18°F*
Gas temperature at cavern top at the end of the choked flow	34°C *94°F*	20°C *68°F*	37°C *98°F*
Ground level temperature at the end of the choked flow	-6°C *21°F*	-27°C *-15.75°F*	-15°C *5°F*
Lowest temperature in the cavern	18°C *65°F*	1°C *34°F*	21°C *70°F*
Lowest temperature at ground level	-19.68°C *-3°F*	-42.12°C *-44°F*	-28°C *-18°F*
Well length or cavern top depth	1,000 m *3,281 ft*	1,000 m *3,281 ft*	1,000 m *3,281 ft*
Gas velocity at cavern top at the starts of blowout	51 m/s *167 ft/s*	155 m/s *509 ft/s*	38 m/s *124 ft/s*
Gas velocity at ground level at the starts of blowout	432 m/s *1,419 ft/s*	1263 m/s *4,142 ft/s*	327 m/s *1,073 ft/s*
Gas velocity at cavern top at the end of the choked flow	50 m/s *164 ft/s*	138 m/s *454 ft/s*	37 m/s *122 ft/s*
Gas velocity at ground level at the end of the choked flow	425 m/s *1,395 ft/s*	1188 m/s *3,897 ft/s*	323 m/s *1,059 ft/s*
Cavern volume	500,456 m^3 *4.2 MMbbls*	500,456 m^3 *4.2 MMbbls*	500,456 m^3 *4.2 MMbbls*
Gas mass	53,407.46 tons *118 MMlbm*	5936.27 tons *13 MMlbm*	96,375.11 tons *212 MMlbm*
Maximum flux from cavern wall	11.94 MW *11,316 BTU/s*	26.54 MW *25,155 BTU/s*	10.58 MW *10,028 BTU/s*
Tubing diameter – internal diameter	*8"5/8* 0.20 m	*8"5/8* 0.20 m	*8"5/8* 0.20 m

Analysis of sensitivity to cavern geometrical characteristics

On this section, the three salt caverns (Cavern#0, Cavern#1 and Cavern#2) filled with hydrogen are used for numerical computations. Results of blowout modeling are compared for those three generic caverns 100,793 m^3 (*0.8 MMbbls*), 500,456 m^3 (*4.2 MMbbls*) and 1,003,163 m^3 (*8.4 MMbbls*), set at the same cavern roof depth, with different tubing diameters: 7"5/8, 8"5/8 and 9"5/8, respectively. There are slight differences between maximum pressure for the gases due to the cylindrical shape of the caverns. It is observed that the cavern volume and the tubing diameter have a real impact on the emptying velocity of the salt cavern and therefore on the blowout duration. Indeed, the salt caverns having a small volume are emptied more quickly. Summary of the results of this analysis on tubing diameter is provided on Table 9.

Table 9. Summary of the results of blowout sensitivity analysis on 3 caverns

Blowout Keys parameters	Cavern#1	Cavern#0	Cavern#2
Blowout duration	2.1 days	7.3 days	11.1 days
Choked flow duration	0.9 days	3.4 days	5.4 days
Normal flow duration	1.2 days	3.9 days	5.7 days
Gas initial pressure	16 MPa *2,409 psi*	17 MPa *2,551 psi*	18 MPa *2,644 psi*
Ground level pressure at the starts of the blowout	1.4 MPa *209 psi*	1.6 MPa *239 psi*	1.8 MPa *263 psi*
Cavern top pressure at the end of the choked flow	1.12 MPa *162 psi*	1.04 MPa *151 psi*	0.98 MPa *142 psi*
Ground level pressure at the end of the choked flow	0.10 MPa *14.7 psi*	0.10 MPa *14.7 psi*	0.10 MPa *14.7 psi*
Gas initial temperature	45°C *113°F*	45°C *113°F*	45°C *113°F*
Ground level temperature at the starts of the blowout	-2.0°C *28°F*	-1.7°C *29°F*	-1.5°C *29°F*
Gas temperature at cavern top at the end of the choked flow	4°C *39°F*	20°C *69°F*	24°C *76°F*
Ground level temperature at the end of the choked flow	-41°C *-41°F*	-26°C *-16°F*	-23°C *-9°F*
Lowest temperature in the cavern	-10°C *13°F*	1°C *34°F*	3°C *38°F*
Lowest temperature at ground level	-52°C *-94°F*	-42°C *-44°F*	-40°C *-40°F*
Well length or cavern top depth	1,000 m *3,281 ft*	1,000 m *3,281 ft*	1,000 m *3,281 ft*
Gas velocity at cavern top at the starts of blowout	143 m/s *468 ft/s*	155 m/s *509 ft/s*	165 m/s *543 ft/s*
Gas velocity at ground level at the starts of blowout	1,260 m/s *4,133 ft/s*	1,263 m/s *4,142 ft/s*	1,265 m/s *4,150 ft/s*
Gas velocity at cavern top at the end of the choked flow	124 m/s *407 ft/s*	138 m/s *454 ft/s*	148 m/s *485 ft/s*
Gas velocity at ground level at the end of the choked flow	1,153 m/s *3,784 ft/s*	1,188 m/s *3,897 ft/s*	1,196 m/s *3,925 ft/s*
Cavern volume	**100,793 m^3** ***0.8 MMbbls***	**500,456 m^3** ***4.2 MMbbls***	**1,003,163 m^3** ***8.4 MMbbls***
Gas mass	1,137 tons *2.5 MMlbm*	5,936 tons *13 MMlbm*	12,271 tons *27 MMlbm*
Maximum flux from cavern wall	14 MW *13,487 BTU/s*	27 MW *25,155 BTU/s*	38 MW *35,723 BTU/s*
Tubing diameter – internal diameter	***7"5/8*** **0.17 m**	***8"5/8*** **0.20 m**	***9"5/8*** **0.22 m**

Joule-Thompson effect

The Joule-Thomson expansion is observed when a real gas (as differentiated from an ideal gas) expands through a throttling device: its enthalpy remains constant. Gas temperature may either decrease or increase. To a certain extent, the lower part of the wellbore is such a throttling device as gas enthalpy there is almost constant. Figure 5 shows the distribution of temperature as a function of depth during the cases study of the analysis of sensitivity to: *a)* well depth; *b)* tubing diameter; *c)* gas type and *d)* cavern volume. In most of these figures, hydrogen temperature increases first when flowing upward at the bottom of the well. Hydrogen expansion is close to isenthalpic because the velocities are still low. The invariant constituted by the sum of the enthalpy and the kinetic energy is almost equal to the enthalpy alone and it is likely that a Joule-Thomson effect occurs. This Joule-Thompson effect is observed in most hydrogen-filled caverns scenarios, except when the cavern volume is small (volume equal to 100,793 m^3 or *0.8 MMbbls*) and located at shallow depth (cavern roof at 250 m or *820 ft*). Hydrogen warms up slightly during such an expansion (constant enthalpy) while natural gas and compressed air cools down.

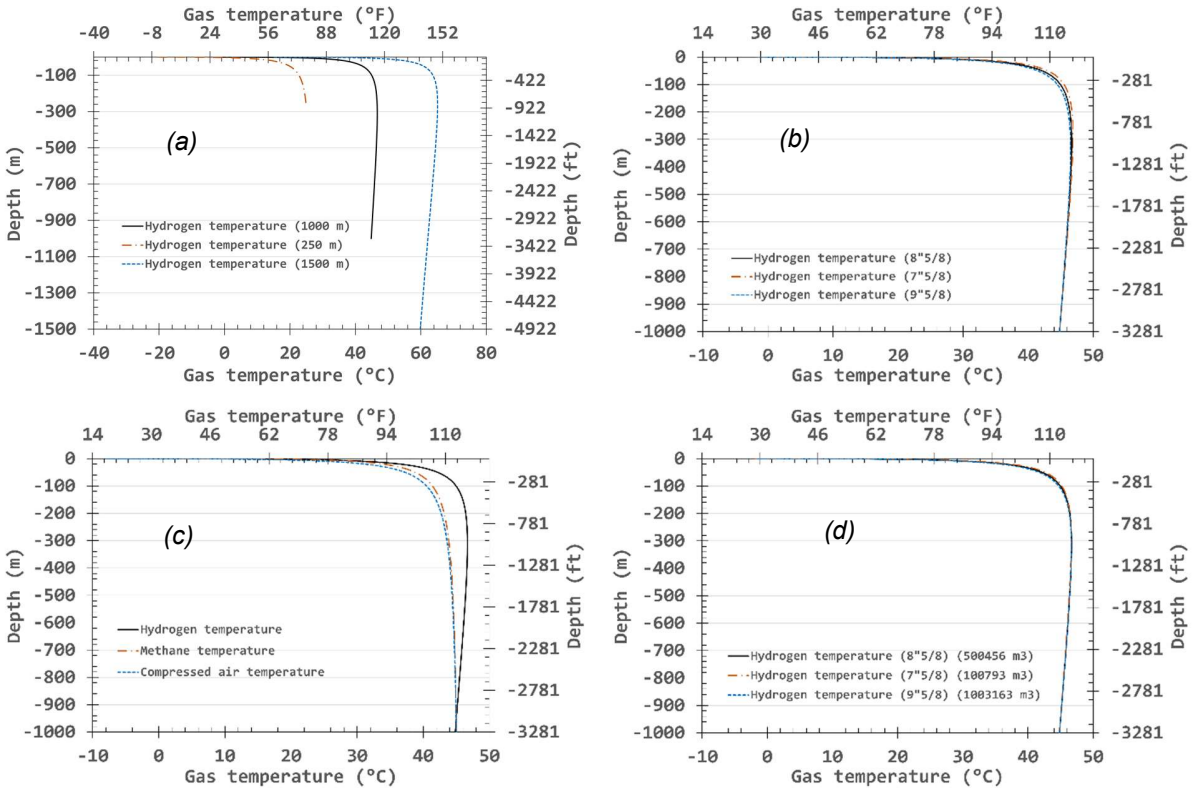

Figure 5. Distribution of temperature as a function of depth at the start of the blowout (t = 0)

Scenario modeling for aerial part of the blowout

The loss of containment that is generated at surface level by a blowout of the Cavern#0, results in the atmospheric dispersion of hydrogen. The assessment of the potential consequences of this hazardous event are evaluated through a computational study of the associated blowout scenario. The purpose of this analysis is to predict not only the concentration profiles generated by the atmospheric gas dispersion but also the thermal and overpressure effects caused by an ignition of the resulting flammable cloud.

Hydrogen atmospheric dispersion

Unified Dispersion Model (UDM)

The Unified Dispersion Model (UDM) was developed by Woodward et al. (1995) to characterize a cloud dispersion developed by a ground-level or elevated two-phase unpressurized or pressurized release. The current version (UDM 3) of this model includes possible plume lift-off, where a grounded cloud becomes buoyant and rises into the air. Rising clouds may be constrained to the mixing layer. This allows assessing the local concentrations of a dispersed gas or vapor after a continuous, instantaneous, constant finite-duration or general time-varying release.

The updated version of the Unified Dispersion Model (UDM 3) is currently implemented in the DNV software application PHAST 8.21. This atmospheric dispersion code has a lower level of complexity than CFD tools, but it can provide more accurate results than approaches based only on Gaussian models. For this reason, it is widely considered for risk assessments.

The numerical scheme of the UDM 3 model is based on a parametrical solution of the fluid mechanics equations. For this purpose, four modules are available for the description of the following scenarios of pollutants dispersion:

- High-pressure releases in which the dispersion is mainly controlled by the kinetic energy of the mixture;
- Dispersions dominated by both the kinetic energy of the release and the gravity effects;
- Dispersions of high-density substances;
- Highly diluted dispersions in which a Gaussian model can be applied due to the neutral buoyancy of the mixture at ambient conditions.

The UDM 3 model provides a description of the general behavior of a pollutant dispersion with a low computational cost. For this purpose, it considers some assumptions about the environment that allow omitting specific details of the scenario without compromising the accuracy of the simulation results. For instance, the terrain is considered to be flat and have a uniform roughness (no obstacles). Moreover, the simulation code assumes that the atmospheric conditions are invariable throughout the discharge.

Additionally, UDM 3 calculates the phase distribution and cloud temperature using either a non-equilibrium thermodynamics model or a non-reactive equilibrium model. These aspects allow the consideration of phenomena such as droplet rainout, pool spreading and re-evaporation (Witlox & Holt, 1999).

Furthermore, a set of ordinary differential equations is integrated into the model for the description of the following dispersion phenomena:

- Conservation of mass (air entrainment and water added from substrate);
- Conservation of momentum;
- Relation between cloud speed and cloud position;
- Heat-transfer relation;
- Water-vapor transfer relation;
- Crosswind spreading.

Atmospheric conditions

In accordance with the French ministerial circular/directive of May 10th, 2010, this modelling of vertical and high releases of hydrogen is carried out for the Pasquill's atmospheric conditions A3, B3, B5, C5, C10, D5, D10, E3 and F3. As a reminder, the Pasquill classification considers two parameters for the atmosphere definition. The letter specifies the atmospheric stability (from A – very unstable – to F – very stable) and the number determines the wind speed (m/s) at a reference height of 10 m (*33 ft*). The values of temperature, humidity and solar radiation, fixed for each condition, are specified as follows:

Table 1 : Meteorological parameters of the Pasquill's atmospheric conditions.

Atmospheric condition	Definition	Ambient temperature	Humidity	Solar radiation
A3	Very unstable Sunny + Light winds	20°C *68°F*	70%	0.5 kW/m^2 *0.044 BTU/ft^2*
B3	Unstable Less sunny or windier than A	20°C *68°F*	70%	0.5 kW/m^2 0.044 BTU/ft^2
B5		20°C *68°F*	70%	0.5 kW/m^2 0.044 BTU/ft^2
C5	Moderately unstable Very windy/sunny or overcast/light wind	20°C *68°F*	70%	0.5 kW/m^2 *0.044 BTU/ft^2*
C10		20°C *68°F*	70%	0.5 kW/m^2 *0.044 BTU/ft^2*
D5	Neutral Little sun and high wind or overcast/windy night	20°C *68°F*	70%	0.5 kW/m^2 *0.044 BTU/ft^2*
D10		20°C *68°F*	70%	0.5 kW/m^2 *0.044 BTU/ft^2*
E3	Moderately stable Less overcast and less windy night than D	20°C *68°F*	70%	0.5 kW/m^2 *0.044 BTU/ft^2*
F3	Stable Night with moderate clouds and light/moderate wind	20°C *68°F*	70%	0.0 kW/m^2 *0.0 BTU/ft^2*

Hazardous events generated by the hydrogen combustion

The hazardous phenomena that might occur due to a hydrogen containment loss are mainly associated with the ignition of the dispersing flammable cloud:

- Flash fire (thermal effects are dominant);
- Unconfined vapor cloud explosion (overpressure effects are dominant);
- Jet fire (thermal effects are dominant).

Flash Fire

The distance of effects of a flash fire are determined by the results of the hydrogen dispersion model according to the following criteria:

- Significant lethal effects = distance to the Lower Flamability Limit (LFL);
- Lethal effects = distance to the LFL;
- Irreversible effects = 1.1 x distance to the LFL.

Unconfined vapor cloud explosion (UVCE)

The evaluation of the effects of the explosion of the unconfined cloud formed by the hydrogen release is carried out according to the multi-Energy method. The method involves estimating the combustion energy available in the various parts of the cloud and assigning to each part an initial strength (Mannan, 2005). For this purpose, the method proposes an integration of experimental data with theoretical predictions of hemispherical gas deflagrations.

The multi-energy method considers a sequential procedure to evaluate the overpressure levels of a UVCE. Firstly, the results obtained with the dispersion model establish the extent of the cloud in the environment.

Then, the concentration profiles of the combustible cloud are used to determine the volumes of fuel-air mixture in the area considered as a blast source. Subsequently, the volume of the equivalent fuel-air charge allows calculating the combustion energy released by the UVCE (Crowl & Louvar, 2011). Finally, a set of empirical equations associate the amount of released energy with the overpressure levels reached by the blast.

Volume of fuel-air mixture:

The calculation of the volumes of fuel-air mixture in the blast zone is performed by taking into account the concentration profiles considered for the evaluation of the flash fire effects.

Explosion severity index:

The estimation of the overpressure levels depends on the assignment of the initial strength of the blast. This definition is considered by the multi-energy method to determine the maximum overpressure. For this purpose, a severity index is selected for the cloud explosion by considering aspects such as the local confinement and the reactivity of the combustible gas.

This severity index is denoted by a number in the range 1-10, where 1 applies to an explosion of insignificant strength and 10 to a detonation (Lees, 2005). The determination of this parameter can be performed according to different approaches based on experimental evidences (Crowl & Louvar, 2011).

Distance of effects:

The distances of effects are determined with the 'multi-energy method' module of the computational tool EPHEDRA, which is developed by INERIS. For this purpose, the following criteria are considered:

- Significant lethal and domino effects = Maximum distance with an overpressure equal or greater than 200 mbar (*3 psi*);
- Lethal effects = Maximum distance with an overpressure equal or greater than 140 mbar (*2 psi*);
- Irreversible effects = Maximum distance with an overpressure equal or greater than 50 mbar (*0.7 psi*).

Jet fire

A jet flame occurs following the ignition of a flammable fluid issuing from a pipe or orifice. By radiation and convection, it dissipates heat which, apart from the visible boundaries of the flame, could be hazardous to life and property.

The DNV software application PHAST 8.21 has implemented various models to evaluate the effects resulting from jet fires generated by gas/vapor releases. In this study, the physical description of vertical and inclined flames is carried out according to the Chamberlain model, which represents them as solid bodies.

Distance of effects:

The distances of effects are determined with the software application PHAST 8.21 according to the following criteria:

- Significant lethal and domino effects = Maximum distance with a thermal radiation equal or greater than 8 kW/m^2 (*0.70 BTU/s ft^2*);
- Lethal effects = Maximum distance with a thermal radiation equal or greater than 5 kW/m^2 (*0.44 BTU/s ft^2*);
- Irreversible effects = Maximum distance with a thermal radiation equal or greater than 3 kW/m^2 (*0.26 BTU/s ft^2*).

Computation of the aerial part of the blowout

Unified Dispersion Model (UDM 3)

Hydrogen atmospheric dispersion

Figure 6 presents the evolution of the dispersion cloud during the hydrogen blowout (total duration = 175.9 hours). In this figure, the contours allow determining the zones with concentrations equal or greater than the hydrogen's lower flammability limit (40,000 ppm). According to the predictions, the maximum expansion of the combustible cloud is achieved during the first 120 minutes of release. Subsequently, plume size decreases due to the pressure drop within the cavern.

The evaluation of the consequences related to the ignition of the flammable cloud was made 120 minutes after the onset of the release. Figure 6A shows the dispersion of the hydrogen cloud depending on the atmospheric conditions. Interestingly, the longest expansion in the downwind direction (34 m or 112 ft) is reached at a height of 40 m (131 ft) when the condition is 10D.

2 min

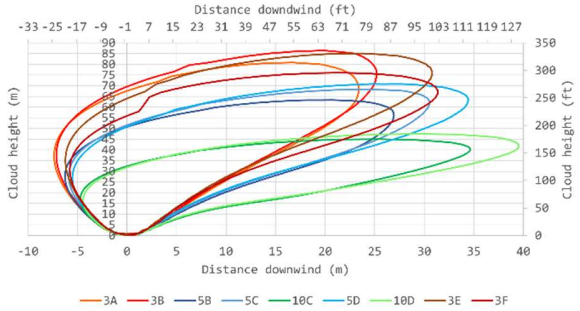

5 min

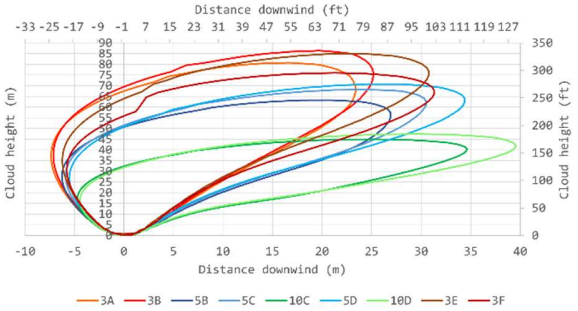

120 min

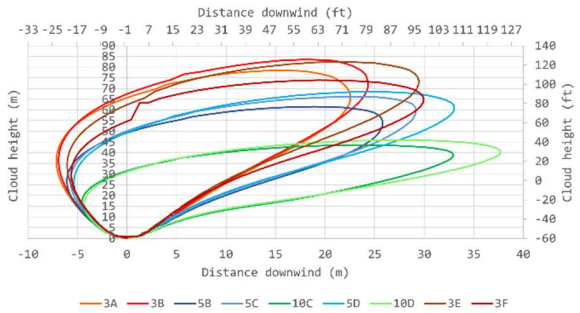

1 day

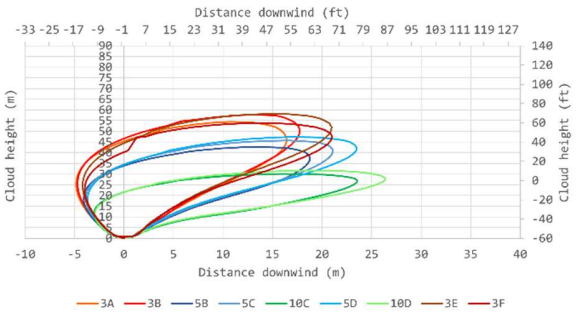

2 days

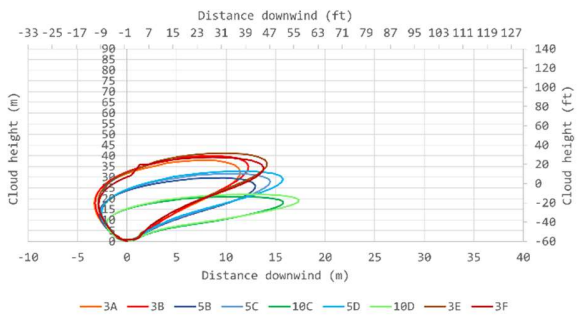

3 days

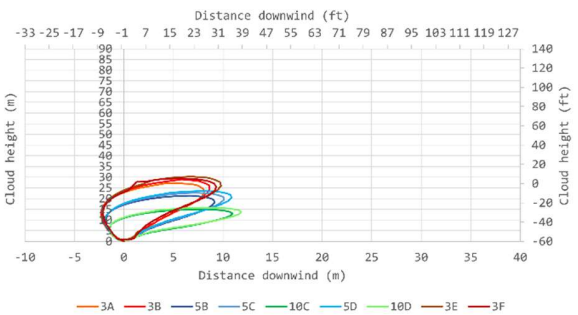

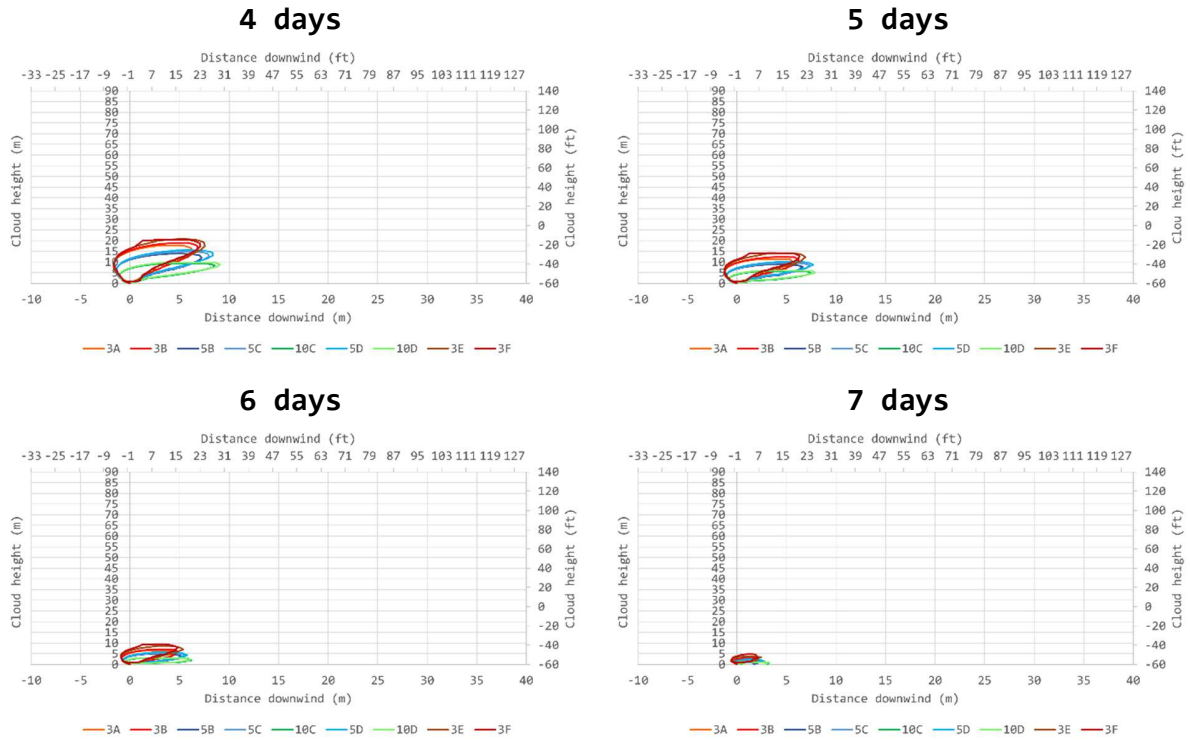

Figure 6 : Evolution of the hydrogen plume formed by a leak in the Cavern#0 (contours: lower flammability limit of hydrogen, i.e., 40,000 ppm).

Evaluation of hazardous events following an ignition of the hydrogen flammable cloud

Flash fire

The distances for a flash fire event in this scenario are presented in Table 2 for the 9 atmospheric conditions considered in this study:

Table 2. Maximum distances of effects for a flash fire after a loss of containment in the Cavern#0.

Threshold	Atmospheric condition								
	3A	3B	5B	5C	10C	5D	10D	3E	3F
Irreversible effects	26.0 m *85 ft*	28.5 m *94 ft*	29.7 m *97 ft*	34.5 m *113 ft*	38.5 m *126 ft*	38.0 m *125 ft*	43.5 m *143 ft*	34.5 m *113 ft*	35.0 m *115 ft*
Lethal effects	23.5 m *77 ft*	25.5 m *84 ft*	27.0 m *89 ft*	31.0 m *102 ft*	35.0 m *115 ft*	34.5 m *113 ft*	39.5 m *130 ft*	31.0 m *102 ft*	31.5 m *103 ft*
Significant lethal effects	23.5 m *77 ft*	25.5 m *84 ft*	27.0 m *89 ft*	31.0 m *102 ft*	35.0 m *115 ft*	34.5 m *113 ft*	39.5 m *130 ft*	31.0 m *102 ft*	31.5 m *103 ft*

Unconfined Vapor Cloud explosion (UVCE)

In accordance with this statement, the volumes are estimated according to the results obtained for the gas dispersion at 120 minutes (7,200 s) (Figure 6*a*). The mass of H_2 in the spherical region located at the middle of each plume is presented below:

Table 3. Mass of H_2 in the spherical region at the middle of the plume generated by a leak in the Cavern#0.

Mass of H_2	Atmospheric condition								
	3A	3B	5B	5C	10C	5D	10D	3E	3F
	1708 kg *3,766 lbm*	1678 kg *3,700 lbm*	653 kg *1,440 lbm*	653 kg *1,440 lbm*	202 kg *446 lbm*	601 kg *1,325 lbm*	190 kg *419 lbm*	1174 kg *2,589 lbm*	954 kg *2,104 lbm*

Explosion severity index:

Figure 7 shows the evolution of the explosion overpressure in an open field as a function of the hydrogen release flowrate. This plot was used to choose the explosion severity because the environment around the cavern's head is an open field with a low confinement level. At the time considered for this calculation, the hydrogen flowrate is above 57 kg/s. Hence, the estimation of the distance of effects is based on a severity index equal to 7.

Distances of effects:

The distances of effects are determined by associating the energy provided by the hydrogen combustion with the maximum distance in which the LFL is reached. In this case, the distances are estimated according to a pressure-distance profile defined for the severity index equal to 7 (van den Berg, 1985). The results are presented in Table 12.

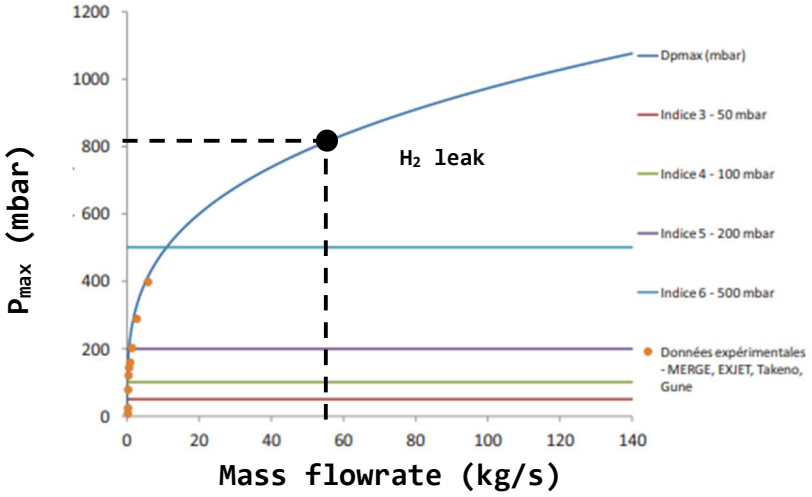

Figure 7 : Explosion overpressure as a function of the mass flowrate of a hydrogen jet (INERIS, 2016).

Table 4 : Distances of overpressure effects generated by an UVCE near the Cavern#0.

Threshold	Pressure	Atmospheric condition								
		3A	3B	5B	5C	10C	5D	10D	3E	3F
Irreversible effects	50 mbar *0.7 psi*	693 m *2,274 ft*	690 m *2,264 ft*	508 m *1,667 ft*	510 m *1,673 ft*	351 m *1,152 ft*	498 m *1,634 ft*	347 m *1,138 ft*	617 m *2,024 ft*	577 m *1,893 ft*

Lethal effects (1%)	140 mbar *2 psi*	310 m *1,017 ft*	309 m *1,014 ft*	229 m *751 ft*	231 m *758 ft*	163 m *535 ft*	227 m *745 ft*	162 m *532 ft*	278 m *912 ft*	261 m *856 ft*
Significant lethal and domino effects (5%)	200 mbar *3 psi*	244 m *800 ft*	244 m *801 ft*	182 m *597 ft*	184 m *604 ft*	131 m *430 ft*	181 m *594 ft*	131 m *430 ft*	220 m *722 ft*	207 m *679 ft*

Jet fire

The evaluation of the radiation effects associated with a jet fire considers the predictive results of the hydrogen atmospheric dispersion. Figure 8 presents the radiation levels of a jet fire at these heights along with the radiation levels at 1.5 m (*5 ft*) in order to evaluate the effects on the general public.

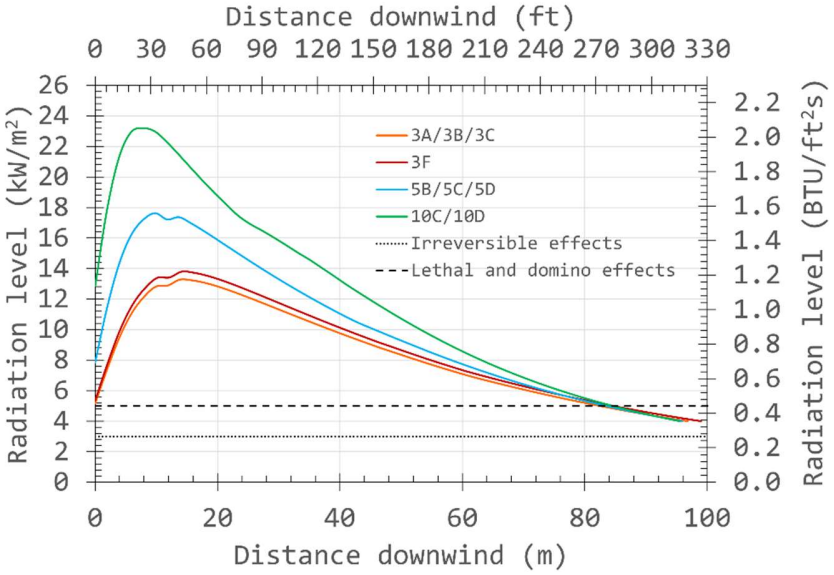

Figure 8 : Radiation levels generated at 1.5 m (*4,92 ft*) by a jet fire in the Cavern#0.

The effects at 1.5 m (*5 ft*) surpass the thresholds defined for the effects on the working personnel and the general public. According to the simulation results, the longest distances of effects are obtained in an atmosphere at the conditions 10C and 10D. The distances of effects are listed in

Table 5.

Table 5 : Distances of thermal effects at 1.5 m (5 ft) generated by a jet fire in the Cavern#0

Threshold	Radiation level	Atmospheric condition			
		3A/B/E	3F	5B/C/D	10C/D
Irreversible effects	3 kW/m^2 *0.26 BTU/ft-s^2*	107 m *351 ft*	110 m *361 ft*	105 m *345 ft*	105 m *345 ft*
Lethal effects (1%)	5 kW/m^2 *0.44 BTU/ft-s^2*	83 m *272 ft*	86 m *282 ft*	85 m *279 ft*	86 m *282 ft*
Significant lethal and domino effects (5%)	8 kW/m^2 *0.70 BTU/ft-s^2*	54 m *177 ft*	55 m *180 ft*	57 m *187 ft*	63 m *207 ft*

Conclusion

A simplified solution was used to compute the evolution of gas pressures, temperatures, and velocities during a blowout in a gas storage cavern. It was shown that, in general, the flow is choked when gas pressure in the cavern is high and is normal when the cavern pressure is low. This model provides a good basis for computation of the thermomechanical behavior of cavern walls during a blowout, a concern of special significance for two reasons: it is important, before a blowout, to establish a credible scenario (gas rate, duration) and, after a blowout, to assess if the cavern can be operated again. The actual validity of the mathematical solution at the end of the blowout is arguable, as water vapor condensation, for instance, may play a significant role.

The loss of containment that is generated at surface level by the blowout of Cavern#0 results in the atmospheric dispersion of hydrogen. The assessment of the potential consequences of this hazardous event are evaluated through a computational study of the associated blowout scenario. The purpose of this analysis was to predict not only the concentration profiles generated by the atmospheric gas dispersion but also the thermal and overpressure effects caused by an ignition of the resulting flammable cloud.

Acknowledgements

This study was funded partially by the European Union in the framework of the Hypster project, which included research conducted by Storengy (France), Armines-Ecole Polytechnique (France), INOVYN (United Kingdom), ESK (Germany), Element Energy (UK), Ineris (France), Axelera (France), Brouard Consulting (France) and Equinor (Norway).

Reference

Bérest P., Brouard B., Hévin G. and Réveillère A. (2021). Tightness of salt caverns used for hydrogen storage. SMRI Spring Virtual Technical Conference, April.

Bérest, P., Brouard, B., Djizanne, H. and Hévin, G. (2014). Thermomechanical effects of a rapid depressurization in a gas cavern. Acta Geotechnica, 9(1), 181–186. https://doi.org/10.1007/s11440-013-0233-8

Bérest, P., Brouard, B., Favret, F., Hévin, G. and Karimi-Jafari, M. (2015). Maximum Pressure in Gas Storage Caverns. SMRI Spring Meeting, Rochester, New York.

Bérest, P., Djizanne, H., Brouard, B. and Frangi, A. (2013). A Simplified Solution For Gas Flow During a Blow-out in an H2 or Air Storage Cavern. Proceedings of SMRI. SMRI Spring Meeting, Lafayette, USA

Brouard, B., Zakharov, V. and Frangi, A. (2020). Full Geomechanical Modeling and Data Management of a Gas-Storage Facility Using LOCAS 3D. Proc. SMRI Fall Virtual Technical Conference.

Crowl, D. A. and Louvar, J. F. (2011). Chemical process safety: Fundamentals with applications. Prentice Hall.

Djizanne, H., Bérest, P. and Brouard, B. (2014). The Mechanical Stability of a Salt Cavern Used for Compressed Air Energy Storage (CAES). SMRI Spring Meeting, San Antonio, TX, USA.

Djizanne, H., Bérest, P., Brouard, B. and Frangi, A. (2014). Blowout in salt caverns. Oil & Gas Science and Technology – Rev. IFP Energies Nouvelles.

INERIS. (2016). Omega UVCE - Les explosions non confinées de gaz et de vapeurs (DRA-16-133610-06190A). https://www.ineris.fr/fr/omega-uvce-explosions-non-confinees-gaz-vapeurs [*in French*].

Kepplinger J., Crotogino F., Donadei S. and Wohlers M. (2011). Present Trends in Compressed Air Energy and Hydrogen Storage in Germany. SMRI Fall 2011 Technical Conference 3–4 October, York, United Kingdom.

Landau L. and Lifschitz E. (1971). Mécanique des Fluides. Éditions MIR. [in French].

Alberta Energy and Utilities Board (2002). BP Canada Energy Company: Ethane Cavern well fires, Fort Saskatchewan, Alberta, Aug./Sept. 2001, EUB post incident report.

Lees, F. P. (2005). Lees' Loss Prevention in the Process Industries (Partially updated by S. Mannan) (Vol. 1-1-3). Elsevier/Butterworth-Heinemann.

Louvet F., Charnavel Y. and Hévin G. (2017). Thermodynamic Studies of Hydrogen Storage in Salt Caverns. SMRI Spring 2017 Technical Conference 23 – 26 April, Albuquerque, New Mexico.

Mannan, S. (2005). Explosion. In S. Mannan (Ed.), Lees' Loss Prevention in the Process Industries (Third Edition) (p. 1-311). Butterworth-Heinemann.

Réveillère A., Bérest P., Evans D., Stöwer M., Chabannes C., Koopmans T., Boly R. (2017). SMRI Research Report RR201-72 Past Salt Caverns Incidents Database Part1: Leakage, Overfilling and Blow-out

Rittenhour T.P. and Heath S.A. (2012). Moss Bluff Cavern 1 Blowout. SMRI Fall Technical Conference, Bremen, Germany, 119-130.

TNO Report R12005 (2020). Inventory of risks associated with underground storage of compressed air (CAES) and hydrogen (UHS), and qualitative comparison of risks of UHS vs. underground storage of natural gas (UGS)

van den Berg, A. C. (1985). The multi-energy method. A framework for vapor cloud explosion blast prediction. Journal of Hazardous Materials, 12(1), 1-10.

Von Vogel P., Marx C. (1985) Berechnung von Blowoutraten in Erdgassonden, Erdoel-Erdgas, 101.Jg, Heft 10, Oktober 1985, 311-316 (in German).

Woodward, J. L., Cook, J., & Papadourakis, A. (1995). Modeling and validation of a dispersing aerosol jet. Journal of Hazardous Materials (2020), 44(2-3), 185-207. https://doi.org/10.1016/0304-3894(95)00054-X